agronomy

Article

# Theoretical and Experimental Verification of the Physical–Mechanical Properties of Organic Bone Meal Granular Fertilizers

Eglė Jotautienė [1,*], Vaidas Bivainis [1], Davut Karayel [1,2] and Ramūnas Mieldažys [1]

[1] Department of Agricultural Engineering and Safety, Faculty of Engineering, Agriculture Academy, Vytautas Magnus University, Studentu Str. 15A, LT-53362 Akademija, Lithuania; vaidas.bivainis@vdu.lt (V.B.); dkarayel@akdeniz.edu.tr (D.K.); ramunas.mieldazys@vdu.lt (R.M.)
[2] Department of Agricultural Machinery and Technologies Engineering, Faculty of Agriculture, Akdeniz University, 07070 Antalya, Turkey
* Correspondence: egle.jotautiene@vdu.lt; Tel.: +370-68086029

**Abstract:** Continuous efforts are being made to improve fertilizer efficiency by improving fertilizer technology, quality, and application rates. Granular organic fertilizers are more difficult to achieve uniform application because their physical–mechanical properties differ significantly from mineral fertilizers. The properties of granular organic fertilizers can best be determined experimentally. However, these studies are often quite complex. Modern engineering modeling software makes it possible to model the properties of granular fertilizers and their dispersion. This study deals with the theoretical and experimental verification of the physical–mechanical properties of organic bone meal granular fertilizer. For the verification of selected properties of bone meal granules, the following studies were carried out on the granules: determination of poured bulk density, static and dynamic angles of repose, static and dynamic friction coefficients of granule surface, etc. The results showed that for modeling fertilizer properties, it is sufficient to carry out a static compression test to determine the modulus of elasticity and a friction test between granules and the contacting surface to determine the static and dynamic friction coefficients. The remaining properties of the granules can be modeled and calibrated with the DEM software Altair EDEM 2023.

**Keywords:** granular fertilizer; physical–mechanical properties; cylindrical form granules; DEM simulation



**Citation:** Jotautienė, E.; Bivainis, V.; Karayel, D.; Mieldažys, R. Theoretical and Experimental Verification of the Physical–Mechanical Properties of Organic Bone Meal Granular Fertilizers. *Agronomy* **2024**, *14*, 1171. https://doi.org/10.3390/agronomy14061171

Academic Editor: Luís Manuel Navas Gracia

Received: 24 April 2024
Revised: 20 May 2024
Accepted: 27 May 2024
Published: 30 May 2024



## 1. Introduction

Recently, there has been growing concern about the consequences of soil fertilizer use. The high use of chemical fertilizers and poor fertilizer application rates deplete resources and pollute the environment, often leading to an excess of hazardous compounds in crops and harming human health [1–4]. Granular organic fertilizers are increasingly used in agriculture due to their lower environmental impact [5,6].

Improvements in fertilizer-spreading technology can lead to the more efficient and rational use of fertilizer, increase fertilizer application rates, enhance food security, and promote sustainable agricultural development [7,8].

In Europe, most organic granular fertilizers are spread using centrifugal disk spreaders. These spreaders are popular due to their low cost and high accuracy. However, the performance of these spreaders and the quality of the fertilizer application are highly dependent on the physical–mechanical properties of the emitted particles [9,10]. Therefore, in the development of fertilizer-spreading technologies, it is essential to investigate the properties of fertilizer in relation to the design of the spreading apparatus, the spreading rates, and the machine set-up [11].

Fulton [12] argues that it is essential to understand the properties of fertilizer particles, such as size, shape, density, and surface roughness. Yule [13] also argues that particle size variation for spreading accuracy is particularly important. Kweon et al. and Zhou et al. suggest that the quality of fertilizer spreading highly depends on factors such as the friction coefficients, Poisson's ratio, particle shape, and density of the spreading particles [9,10]. Thus, the physical–mechanical properties have a significant influence on particle dispersion in soil [13]. Knowing the physical properties of specific fertilizers allows for the accurate identification and calibration of spreaders. Proper machinery setting is essential for achieving a uniform spreading pattern and optimizing crop growth and yield.

For more accurate, faster, and cheaper fertilizer-spreading research, researchers propose the use of modeling based on the discrete element method (DEM) [10,11,14–17]. It is a promising and convenient method to record the dynamic behavior of agricultural materials in the operation of agricultural machinery from both the macro and micro perspectives [17–21].

The researchers modeled the flow of cylindrical particles driven by the rotating disk of a centrifugal spreader (300–650 rpm) using the DEM. The DEM simulations showed good qualitative and significant quantitative agreement with experiments. Errors between the simulation and experimental results were identified as underestimation of the simulated particle velocities at the disk edge and underdispersion of the simulated particle velocities at the disk edge. The researchers argued that it is important to estimate the dynamic friction coefficient, as well as to determine the cause of the unknown externalities that occur at higher disk velocities [11]. Yinyan et al. [2] evaluated the performance of a fertilizer centrifugal spreader in DEM and experimental studies. They reported that a relative error of 10.66% was obtained concerning the simulation results, thus confirming the accuracy of the model. Other researchers report that the experimental results were within the error range of the simulation results, with deviation values of 8.11% and 9.01% for the transverse and longitudinal fertilizer uniformity coefficients, respectively [22].

Zinkevičienė et al. [23] believe that understanding the physical–mechanical properties helps optimize spreading efficiency. The simulation results showed that a more uniform distribution of organic granular fertilizers on the soil surface was obtained due to shorter granule length, larger diameter, lower density, and higher mass. However, in practice, many fertilizer properties that are not included in the model affect the fertilizer flow, and therefore, it is necessary to calibrate the simulation models for each type of fertilizer [24].

The aim of this work is to determine the physical–mechanical properties of organic cylindrical bone meal granular fertilizers through experimental investigation, verifying the obtained results with the simulation results from the DEM simulations, and evaluate the differences in the properties and behavior of spherical granules in comparison to cylindrical granules to gain comprehensive knowledge and increase fertilizer use efficiency.

## 2. Materials and Methods

Modeling the behavior of different forms of organic fertilizer granules using the discrete element method (DEM) is complex and challenging. This modeling requires knowledge of the geometrical characteristics of the granules, the material properties of the granules and the test equipment, and the interaction properties between the granules and the test equipment. The experimental determination of all these properties of the test granules is quite complex and requires a lot of time and laboratory equipment resources. It is sufficient to determine a few key properties for the modeling during the tests while the remaining values are selected and calibrated.

The experimental investigations have led to the determination of the geometrical characteristics of the cylindrical bone meal granules and the calculation of the material density of the granules. The modulus of elasticity of the granules is one of the most important properties required in DEM simulation. Therefore, static compression tests were carried out on the cylindrical granules to determine the modulus of elasticity of the granules. In addition, experimental investigations were carried out to determine the properties of the interaction between the granules and the test equipment, such as the static and dynamic (or rolling) coefficients of friction between the granules and the surface in contact with them. The remaining values of the interaction properties of the granules and granules relevant for DEM simulation, i.e., not experimentally determined, were taken from the results of similar studies [8,25–27] and calibrated. It is worth noting that no similar studies on cylindrical granules could be found here. Experimental investigations were carried out to determine the values of the dynamic angle of repose of cylindrical bone meal granules and the height of the granules' bed, the static angle of repose, and the bulk density to obtain the smallest possible errors between experimental and simulation results. Analogous modeling studies on the properties of cylindrical granules were performed to calibrate the particle property values of the granules required for DEM simulation.

Recently, there has been a growing demand for spherical organic granular fertilizers in the organic granular fertilizer market due to the more uniform spreading characteristics of standard centrifugal spreaders and the possibility of incorporating additional substances and formulations during granulation. In this research, DEM simulation studies were carried out on spherical bone meal granules, identical to cylindrical bone meal granule material, to assess the properties and behavior of spherical granular fertilizers. The aim of these studies was to assess the differences in properties and behavior of spherical granules compared to cylindrical granules.

The diameter and length of the cylindrical bone meal granules were determined by measuring 100 randomly selected granules. The measurements were carried out using a Mitutoyo 500-196-30 electronic caliper (Mitutoyo, Kanagawa, Japan) with a graduation of 0.01 mm. The material density of these granules was calculated from the measured length, diameter, and weight of the granules. The weight of the granules was determined using a Kern EWJ electronic laboratory (Kern&Sohn GmbH, Ebingen, Germany) balance with a division of 0.01 g.

The modulus of elasticity or Young's modulus of the bone meal granules was determined using strength tests. Organic bone meal granules' strength tests were performed in a 5 kN capacity test machine, Instron 5960 (ITW, Norwood, MA, USA), and the parameter registration software system Bluehill (version 3.11.1209). The granules were placed horizontally and vertically on the center of the circular plate and individually compressed until breakage was achieved. Granule compressive strength (N) was determined as the maximum force recorded when compressing the granule at fracture. The limiting force (load, N) and extension (deformation, mm) were recorded at that moment. This test was performed by compressing the granule with a 7.92 mm die at a speed of 20 mm·min$^{-1}$. Such a load is considered semi-static since the effect of inertia is insignificant. Tests were repeated ten times for each sample of bone meal granules in horizontal and vertical directions. The Instron Bluehill compression application module contains all the necessary set-up parameters, and Young's modulus, MPa, has been calculated.

MS Office Excel 2007 was used to analyze the experimental results statistically. During all data processing, using the appropriate number of repetitions, average values, and mean values with the 95% confidence interval of the mean and the least significant difference $LSD_{05}$ were calculated using a t-test at a probability $p \leq 0.05$ [28].

Calibration studies on the properties of cylindrical and spherical granules were conducted using equipment made of high-density polyethylene (HDPE). The main properties of this material [29] are presented in Table 1.

**Table 1.** Material properties of the equipment.

| Properties | Parameter |
|---|---|
| Material density, kg m$^{-3}$ | 950.00 |
| Young's modulus, MPa | 600.00 |
| Poisson's ratio | 0.45 |

During all tests, the equipment material was in contact with the granules, resulting in the determination of the static and dynamic coefficients of friction between the granules and this polymer. These tests were carried out using the horizontal peel, tear, and friction tester FPT-H1, part of which is shown in Figure 1a.

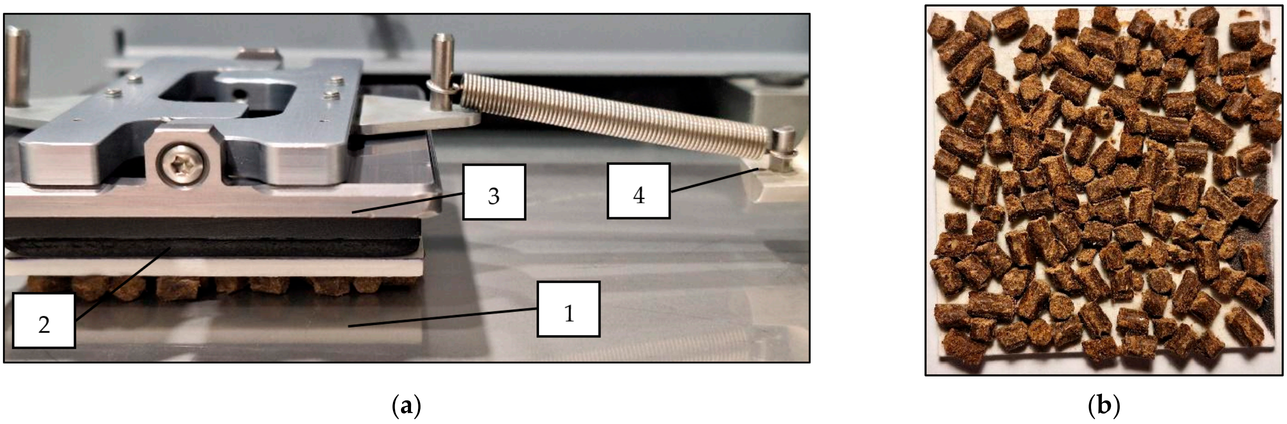


**Figure 1.** Determination of static and dynamic coefficients of friction between the granules and the surface of the equipment; (**a**) view of a part of the friction coefficient determination apparatus: 1—the sub-surface of the material contacting the granules, 2—the tensile test specimen with the granules attached, 3—the weight bearing the granules, and 4—the force-measurement cell; (**b**) image of granules.

The bone meal granules were glued to a 63.5 $\times$ 63.5 mm foamed lightweight polymer plate during the studies. The surface of the glued granules in contact with the test surface was ground to obtain a larger and flatter contact surface. Visually, the granule material covered approximately 75% of the total contact area. During the studies, the specimen was clamped with a mass weight of 200 $\pm$ 2 g and moved at a speed of 150 mm/min. The test lasted 54 s, during which the displacement of the specimen was approximately 135 mm. The test resulted in load-displacement relationships for the specimen to be stretched, and the static and dynamic coefficients of friction of the contacting surfaces were calculated using the specialized Emperor software 1.18 of the apparatus. According to the test methodology, the static coefficient of friction was measured during the first two seconds of the test; the dynamic coefficient of friction was recorded during the remainder of the test.

The above studies have identified the properties of the granules that have the greatest impact on their behavior during experiments and modeling as follows: the material density, the modulus of elasticity of the material, and the static and dynamic coefficients of friction between the granules and the contacting surface. To verify the properties of the selected cylindrical and spherical granules, three experimental studies were carried out to determine the dynamic angle of repose and the height of the granules' bed, the static angle of repose, and the bulk density of the poured granules.

The dynamic angle of repose and the height of the granules' bed were determined using a rotating drum with an internal diameter of 103.39 mm, a drum depth of 75.00 mm, and a volume of 0.63 L. During the tests, the drum was filled with 167.12 g of granules, i.e., approximately 36.42% of its total volume was filled with granules. The drum rotated clockwise at a speed of 1.88 rad $s^{-1}$ for a rotation time of 90 s. The front wall of the drum was transparent, and the dynamic angle of repose and the height of the granules' bed from the bottom of the drum were measured from the footage. These measured parameters are shown in Figure 2a below.

The angle of natural repose of the granules was determined using a bottom ring with a height of 18.00 mm and a ring inner diameter of 103.39 mm. During the tests, a pile of granules was formed in the ring when the granules were poured freely from the top and the angle of repose of the pile was measured. The pellets were formed by pouring the pellets from a container with a diameter of 130 mm, i.e., larger than the ring at the bottom. The container was 150 mm above the ring, and 700 g of pellets were poured in order to form a realistic pile, i.e., more pellets were poured than were needed to fill the ring and form the pile. These edgewise scattered pellets are not shown in the experimental and simulation results. The angle was measured with a protractor with a pitch of 1°. The parameters measured in this study are shown in Figure 2b below.

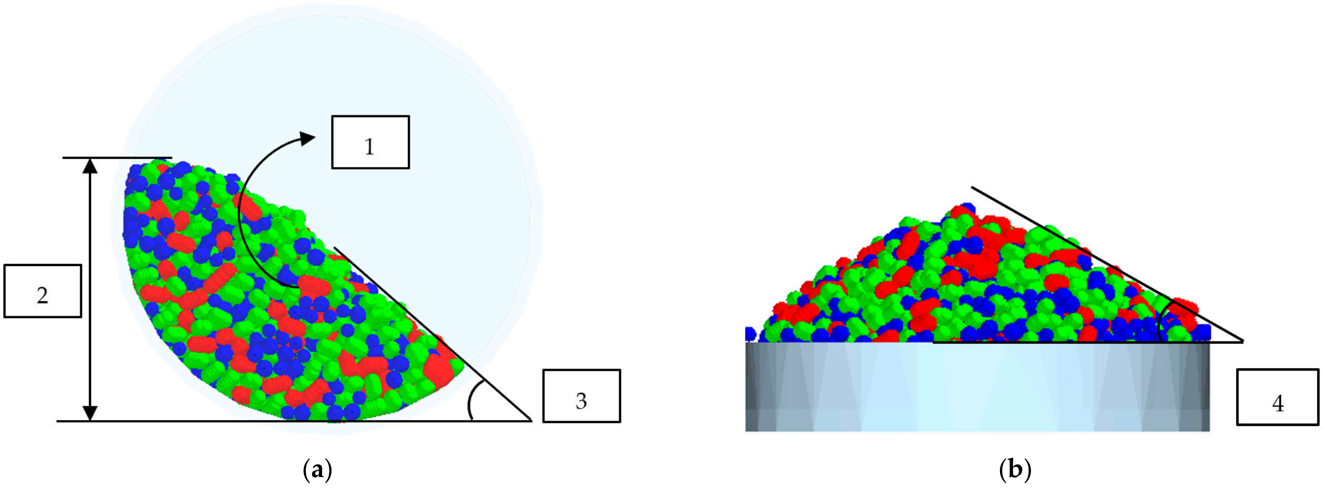


**Figure 2.** Determination of the dynamic granule angle of repose, the height of granules' bed and the static angle of repose; (**a**) determination of the dynamic angle of repose and the maximum height of the granules' bed: 1—the direction of rotation of the drum, 2—the height of the granules' bed, and 3—the dynamic granule angle of repose; (**b**) determination of the static granule angle of repose: 4—the static angle of repose.

The bulk density of the poured granules was determined using a cylindrical vessel with an internal diameter of 103.39 mm, a height of 170.00 mm, and a volume of 1.43 L. The bulk density of the poured granules was calculated by measuring their mass. The setting drum of the dynamic angle of repose, the setting ring of the natural angle of repose, and the bulk density vessel were made from the same 3.00 mm thick HDPE plastic with the properties shown in Table 1.

In all the modeling results, the different color of the particles indicates the different volumes of the granules. The particles with the smallest volume are shown in blue, the particles with the largest volume are in red, and the particles with the medium volume are in green. The experimental studies consisted of at least 5 trials each. The test pieces were kept for about 24 h before the tests at an ambient temperature of about 20 °C and about 50% humidity. The confidence interval for the values obtained was calculated at $\alpha = 0.05$.

The modeling studies on the properties of cylindrical and spherical granules were carried out using the DEM software Altair EDEM 2024. The 3D computer models of the experimental equipment used for the DEM simulations were created using SolidWorks 2024 EDU.

## 3. Results

### *3.1. Granule Geometry*

The diameter of the cylindrical bone meal granules used in the experimental studies was 4.17 ± 0.01 mm. As the confidence interval for the diameter is only 0.01 mm, this is a sufficiently constant value, and this diameter was fixed in the subsequent simulation studies. A histogram of the length distribution of the cylindrical granules is shown in Figure 3a. As can be seen from this histogram, the distribution of the granule lengths is almost symmetric; the kurtosis of the data was −0.16, and the skewness was 0.32. The minimum value was 3.00 mm, the maximum value was 10.27 mm, and the range was 7.27 mm. The dispersion of the granule lengths is large, and therefore, seven particle models with different shapes and parameters were used in the DEM simulation studies. The average particle model length, shape, and proportion of different particle models were used from this histogram.

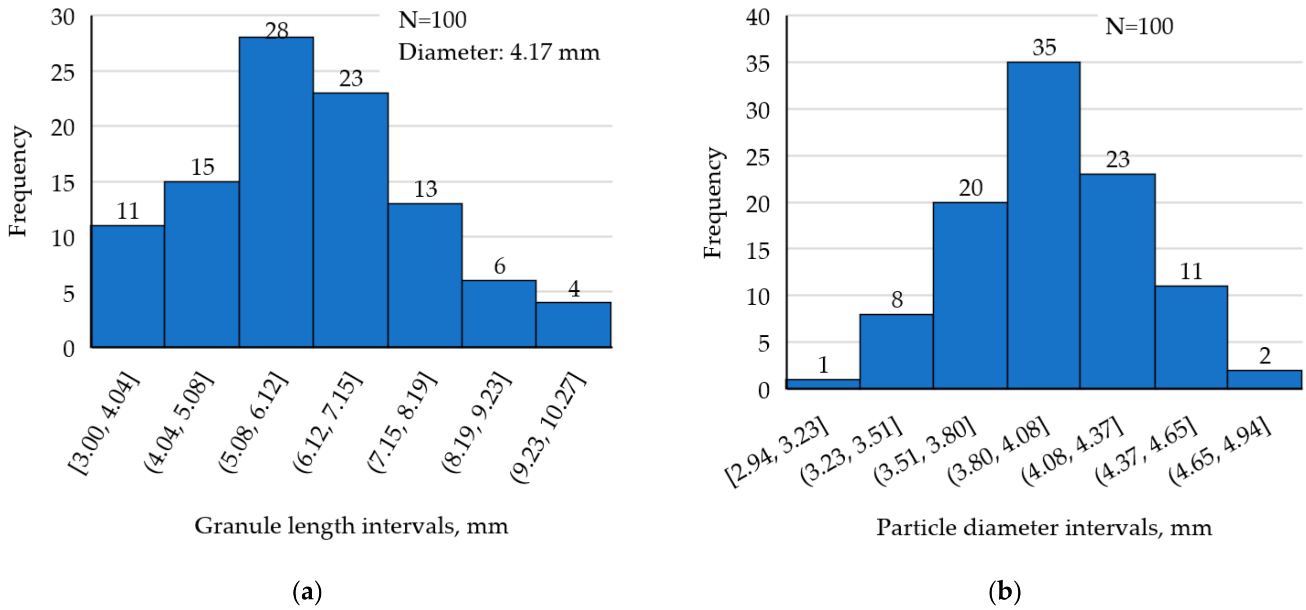


**Figure 3.** Histograms of the distribution of the length and diameter of the granules used in the experimental and simulation studies; (**a**) distribution of the length of the cylindrical granules used in the experiment and the simulation; (**b**) distribution of the diameter of the spherical particle models used in the simulation.

The diameter of the spherical bone meal granules used only in simulation studies was 3.97 ± 0.07 mm. The histogram of the diameter distribution of the spherical beads is shown in Figure 3b. As can be seen from these data, the distribution of the diameter of the granules was symmetrical and close to the Normal Law. The kurtosis of the data was 0.27, and the skewness was 0.15. The minimum value was 2.94 mm, the maximum value was 4.94 mm, and the range was 2.00 mm. These data were used to generate spherical fertilizer particle models.

### *3.2. Granule Strength Properties*

Granule strength ensures that fertilizer will arrive at its destination as intended and can be used without breaking down into finer particles. The strength test curves of bone meal granules, on purpose, show the character of the force variation in the strength test for granules, as shown in Figure 4. The mentioned granules deformed at a maximum compression force of more than 40 N. When analyzing the deformation curves, it was observed that the maximum crushing force in the horizontal direction was from 30.91 to 43.42 N, with deformation ranging from 0.14 mm to 0.23 mm until the granules are completely disintegrated. When analyzing the deformation curves, it was observed that the maximum crushing force in the vertical direction was from 18.10 to 40.76 N, with deformation ranging from 0.43 mm to 0.66 mm until the granules were completely disintegrated. In the vertical direction, the granules did not disintegrate immediately due to their elasticity properties. It can be observed that the fertilizer granules have significant differences in compressive strength, but the compressive failure characteristics are similar. In the early stage of loading, the relationship between the compression force and deformation of the fertilizer grain is almost linear, indicating that the fertilizer granules are elastic in this stage. When the compressive force on the fertilizer granules reaches a peak value, cracks will appear on the fertilizer granules. They would rapidly develop and connect, which would cause the splitting of the granules, resulting in a rapid reduction in compression force.

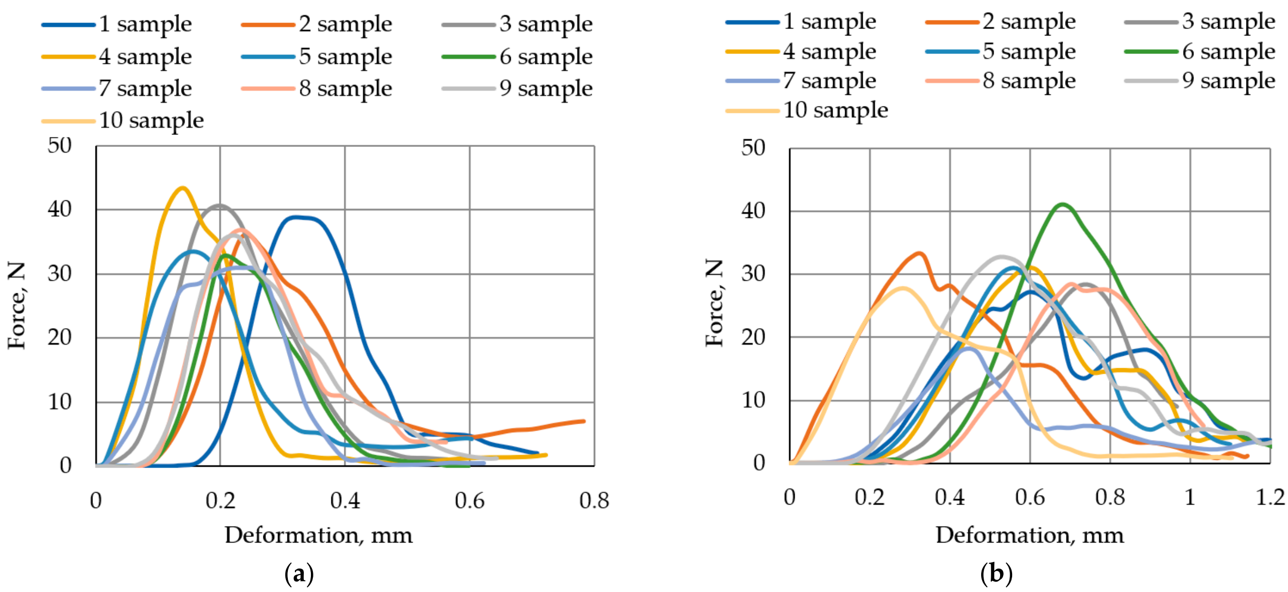


**Figure 4.** Compressive force-deformation curve of fertilizer granules. Curves of granule strength test (**a**) in horizontal direction; (**b**) in vertical direction.

The experimental results presented in Figure 5 show the average strength of the bone meal granules, with a semi-static stability of 36.76 ± 2.81 N in the horizontal direction and 29.81 ± 4.09 N in the vertical direction. There is a significant difference between the forces acting on the granules in horizontal and vertical directions; the granules withstood significantly lower forces under vertical load.

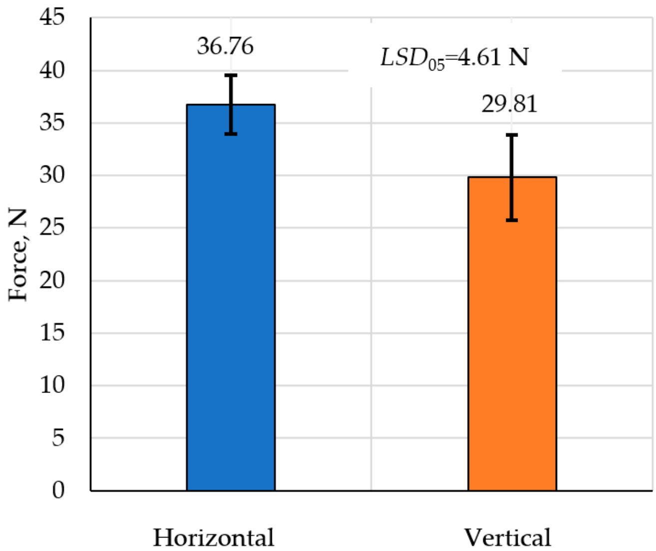


**Figure 5.** Comparison of the compressive strength in horizontal and vertical directions of organic bone meal granular fertilizers. Error bars represent the 95% confidence interval of the mean. A *t*-test was used for statistical analysis.

During the experiments, Young's modulus, MPa, was also determined, which was used later for the simulation. The Instron Bluehill compression application contains various set-up parameters and there was calculated Young's modulus. Using Bluehill software (version 3.11.1209), the average Young's modulus was determined to be 28.82 ± 4.65 in the vertical direction (Table 2).

**Table 2.** Geometry and material properties of cylindrical granules.

| Properties | Parameter |
|---|---|
| Granule diameter, mm | 4.17 ± 0.01 |
| Granule length, mm | 6.07 ± 0.31 |
| Minimum length, mm | 3.00 |
| Maximum length, mm | 10.27 |
| Material density, kg m$^{-3}$ | 1208.98 ± 17.50 |
| Granules' poured bulk density, kg m$^{-3}$ | 728.68 ± 36.43 |
| Young's modulus, MPa | 28.82 ± 4.65 |
| Poisson's ratio | 0.25 * |

* Data were obtained from sources [26] and calibrated.

### *3.3. Granules' Interaction Properties*

The frictional load-displacement relationship for horizontal tension of cylindrical bone meal granules is shown in Figure 6a. This shows the average curve for all experimental results. According to the study methodology, the static coefficient of friction between the two contacting surfaces was recorded during the first 2 s, and here, it can be seen that the nature of the dependence is close to a straight line. From about 2 s onwards, the dynamic coefficient of friction between the contacting surfaces has been recorded, where the friction load values fluctuate. However, the variation is in a range of relatively small values. The adjacent Figure 6b shows the values of the static and dynamic coefficients of friction calculated by the software, together with their scatter.

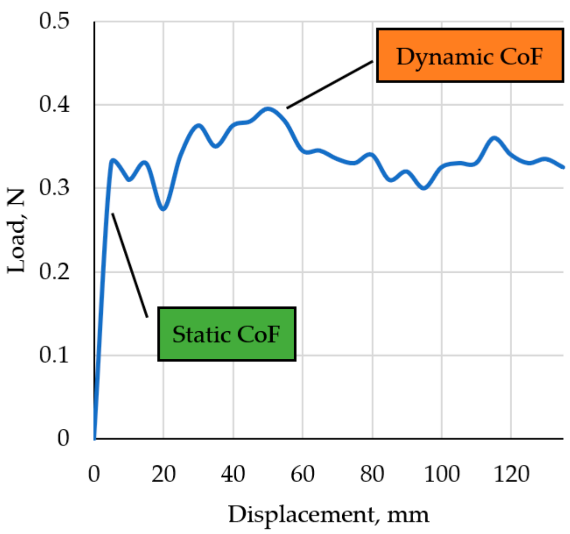


(**a**)

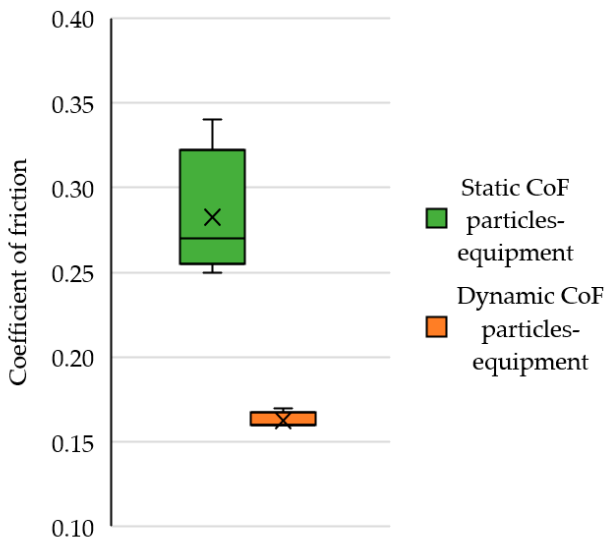


(**b**)

**Figure 6.** Experimental results of friction load and static and dynamic coefficients of friction of cylindrical granules; (**a**) friction load-displacement relationship; (**b**) values of the static and dynamic coefficients of friction between the granules and the equipment surface.

This shows that the dispersion of static coefficients of friction data is significantly larger than that of the dynamic coefficients of friction. This could be due to the heterogeneous nature of the bone granule material, which is composed of particles of different sizes and frictional properties. The different properties of these constituent particles and other surface properties have influenced the wide dispersion in these data.

The properties of the cylindrical bone meal granules determined from the experimental studies are presented in Table 2.

The Poisson's ratio of the material in this table has not been determined in the experiments, but its value has been calibrated during the DEM simulation.

### *3.4. Granule Property Calibration*

The accepted properties of the cylindrical granules, which were not experimentally determined, were calibrated. The shape of the particles used in the DEM simulation, as well as their images, geometric properties, and percentage compositions are presented in Table 3.

**Table 3.** Geometry, shape, and fraction of modeling fertilizer particles.

| Shape | | Length, mm | Diameter, mm | Proportion, % |
|---|---|---|---|---|
| Single-sphere | 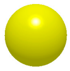 | 3.52 | 3.52 | 11.00 |
| Dual-sphere | 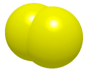 | 4.56 | | 15.00 |
| | | 5.60 | | 28.00 |
| Straight Four Sphere | 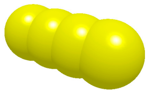 | 6.64 | 4.17 | 23.00 |
| | | 7.67 | | 13.00 |
| | | 8.71 | | 6.00 |
| | | 9.75 | | 4.00 |

As can be seen from this table, the smallest particles, which accounted for 11.00% of the total volume, were in the form of a single sphere, while the rest were in the form of dual or four straight-lined spheres. The behavior of granules and other bulk materials of similar geometry is quite accurately modeled by DEM using particles of this exact shape [26,30]. The simulation uses the Hertz–Mindlin model for the interaction of granules with each other and with granules on contacting surfaces, in which the particles do not stick to each other and to the equipment surface.

Table 4 below shows the properties of the interactions between the granules. Some of these properties were obtained from experimental studies, while others were adopted and calibrated.

**Table 4.** Interaction properties of particles and equipment.

| Interaction | Particle–Particle | Particle–Equipment |
|---|---|---|
| Coefficient of restitution | 0.60 (Range: 0.5~0.7; step 0.10) | 0.45 (Range: 0.35~0.55; step 0.10) |
| Coefficient of static friction | 0.35 (Range: 0.25~0.45; step 0.10) | 0.28 ± 0.04 * |
| Coefficient of dynamic friction | 0.10 (Range: 0.05~0.25; step 0.10) | 0.16 ± 0.005 * |

* Values from the experiments.

In the DEM simulation studies of the properties of the granular particles, the assumed properties were varied by step within a specified interval. First, a calibration study of the static and dynamic coefficients of friction between the granules was carried out. This was performed primarily because these properties (in addition to those already determined from experiments) have the greatest influence on the behavior of the granules (e.g., transport, storage, and spreading by centrifugal fertilizer spreaders). To calibrate these properties, the first and most comprehensive study method was chosen as follows: the determination of the dynamic angle of repose and the height of the granules' bed during the rotation of the granule-filled drum.

In the simulation studies of the dynamic angle of repose and the height of the granules' bed, the particle flow was 16.71 g $s^{-1}$. During the first 10 s, the drum did not rotate as particles were generated. During this time, 167.12 g of particles were generated, the same as in the experiment. The particle-filled drum was then rotated for 20 s. The whole test lasted 30 s. In the first part of the modeling, the static coefficient of friction between the particles was changed from 0.25 to 0.45. The value of the dynamic coefficient of friction between the particles was kept constant at 0.10. The modeling and experimental results are shown in Figure 7a.

| | | | | |
|---|---|---|---|---|
| Dynamic CoF particle–particle (fixed): 0.1 | | | | |
| Static CoF particle–particle (variable) | 0.25 | 0.35 | 0.45 | Experiment |
| Tumbling state | 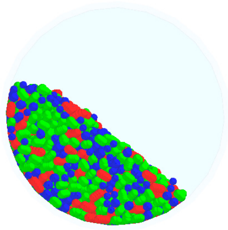 | 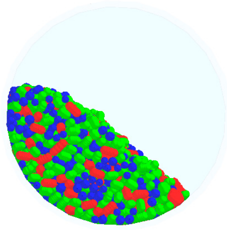 | 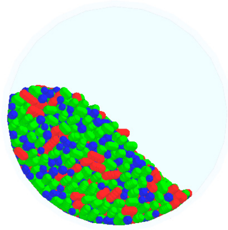 |  |
| Dynamic angle of repose, ° | 38.92 (−0.51% vs. experiment) | 38.35 (−1.97% vs. experiment) | 43.28 (+10.64% vs. experiment) | 39.12 ± 1.26 |
| Height of granules' bed, mm | 68.71 (+4.66% vs. experiment) | 65.64 (+0.20% vs. experiment) | 63.70 (−2.84% vs. experiment) | 65.51 ± 1.75 |
| (**a**) | | | | |
| Static CoF particle–particle (fixed): 0.35 | | | | |
| Dynamic CoF particle–particle (variable) | 0.05 | 0.10 | 0.15 | Experiment |
| Tumbling state | 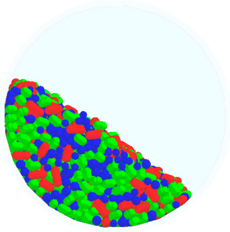 | 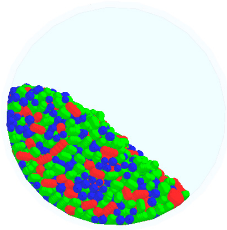 | 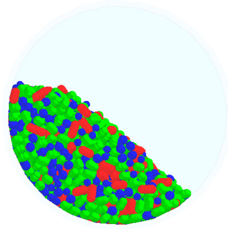 |  |
| Dynamic angle of repose, ° | 34.73 (−11.23% vs. experiment) | 38.35 (−1.97% vs. experiment) | 40.84 (+4.40% vs. experiment) | 39.12 ± 1.26 |
| Height of granules' bed, mm | 69.72 (+6.04% vs. experiment) | 65.64 (+0.20% vs. experiment) | 65.32 (−0.29% vs. experiment) | 65.51 ± 1.75 |
| (**b**) | | | | |

**Figure 7.** Modeling and experimental results of the dynamic angle of repose and the height of the formed granules' bed for cylindrical granules; (**a**) determination of the dynamic angle of repose and the height of the granules' bed under a fixed dynamic coefficient of friction (0.10) between the granules and a variable dynamic coefficient of friction (0.25 ÷ 0.45); (**b**) determination of the dynamic angle of repose and the height of the granules' bed with a variable (0.05 ÷ 0.15) dynamic coefficient of friction between the granules and a fixed (0.35) static coefficient of friction between the granules.

As can be seen from the DEM simulation results presented here, the results closest to the experiment in terms of dynamic angle of repose and height of granules' bed were obtained when the static coefficient of friction between particles was 0.35. At a lower value of the static coefficient of friction, it can be assumed that a readily identifiable granule bed did not form and that the resulting bed height was significantly higher. At higher values of the static coefficient of friction, a visually "longer" granule bed and a granule ridge started to form in the center of the drum, with a significantly higher dynamic angle of repose obtained. From these studies, it can be stated that the lowest difference compared to the experimental results was obtained when the static coefficient of friction between the granule particles was 0.35.

In the next part of the DEM simulation, the static coefficient of friction between the cylindrical granules was fixed at 0.35. The value of the dynamic coefficient of friction varied between 0.05 and 0.15. The best agreement was obtained with a value of this friction coefficient of 0.10. At a lower value, the difference in the dynamic angle of repose was significant, and it can be concluded that no granule bed was formed. At a higher value of the dynamic coefficient of friction between the granules, a significantly larger granules' bed was formed, and the height of the granules' bed was significantly higher compared to the experimental results.

Calibration studies on the properties of the granules' static angle of repose were carried out in a similar sequence. The DEM simulation of the natural granules' static angle of repose resulted in a particle flow of 45.00 g $s^{-1}$ and a simulation time of 23 s. The results of the experimental and modeling studies are shown in Figure 8 below.

| Dynamic CoF particle–particle (fixed): 0.1 | | | | |
|---|---|---|---|---|
| Static CoF particle–particle (variable) | 0.25 | 0.35 | 0.45 | Experiment |
| Tumbling state | 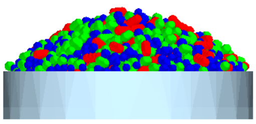 | 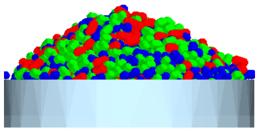 | 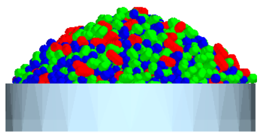 |  |
| Static angle of repose, ° | 27.36 (−6.92% vs. experiment) | 28.64 (−2.58% vs. experiment) | 33.27 (+11.62% vs. experiment) | 29.40 ± 1.71 |

**Figure 8.** Modeling and experimental results of the static angle of repose for cylindrical granules. The dynamic coefficient of friction between the granules was fixed (0.10), and the static coefficient of friction between the granules was variable (0.25 ÷ 0.45).

In the first part of this study, the dynamic coefficient of friction between the granules was kept constant at 0.10, and the static coefficient of friction was varied. The simulation data with a static coefficient of friction of 0.35 were found to be the closest to the experimental results in terms of the shape of the pile of poured granules and the measured values of the angles of repose. At a lower value, the static angle of repose decreased significantly, and at a higher value, the static angle of repose increased. At a fixed value of (0.35) for the static coefficient of friction, but varying for the dynamic coefficient of friction, no significant differences were found between the static angles of repose (and therefore, these data are not presented here).

Similarly, calibration studies on the bulk density properties of cylindrical granules were carried out. In the DEM simulation of the granule bulk density, the flow of the generated granules was 94.55 g $s^{-1}$, and the simulation time was 10 s. By varying the values of the static and dynamic coefficients of friction between the granules, the difference between the modeling results and the experimental results was up to 2.50%. The best agreement between modeling and experimental results was obtained when the static coefficient of friction between the granules was 0.35, and the dynamic coefficient of friction was 0.10. At these values, the mass of the granules obtained in the modeling was 1.04 kg, which was −0.48% less than the experimental mass. The bulk density of the modeled granules was 727.00 kg $m^{-3}$, which was 0.23% less than the experimental result. An almost perfect agreement of results was obtained in these studies.

At these values of the coefficient of friction, analogous calibration studies were carried out on the properties of the granules by varying the values of the coefficient of restitution between the granules and between the granules and the contact surface (as shown in Table 4) and there were no significant differences between the values of the coefficients. The best agreement between modeling and experimental results was obtained with a value of

0.60 for the intergranular coefficient of restitution and 0.45 for the coefficient of restitution between the granules and the surface. Due to the negligible effect of these coefficients on the calibrated granule properties, the modeling results are not presented here.

To determine the behavior of spherical granules that were granulated from the same raw material and to compare their properties with cylindrical granules, modeling studies were carried out on the properties of spherical granules. The results of these studies were compared with the experimental results of cylindrical granules. The results of the studies are presented in Figure 9 below.

| Particle/granule shape | Sphere shape (simulation) | Cylinder shape (experiment) | Sphere shape (simulation) | Cylinder shape (experiment) |
|---|---|---|---|---|
| Tumbling state | 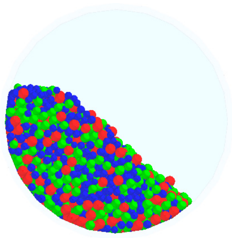 |  | 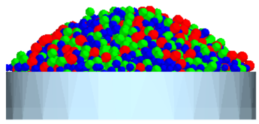 |  |
| Dynamic/static angle of repose, ° | 40.97 (+4.51% vs. experiment) | 39.12 ± 1.26 | 28.62 (−2.64% vs. experiment) | 29.40 ± 1.71 |
| Height of granules' bed, mm | 66.37 (+1.29% vs. experiment) | 65.51 ± 1.75 | | |
| (**a**) | | | (**b**) | |

**Figure 9.** Modeling and experimental results for the determination of dynamic and static angles of repose and the height of the granules' bed for single-sphere and cylindrical granules; (**a**) determination of the dynamic angle of repose of the spherical and cylindrical granules and of the granules' bed that is formed; (**b**) determination of the static angle of repose of spherical and cylindrical granules.

Modeling studies showed that the dynamic angle of repose of the cylindrical granules was about 4.51% higher than the dynamic angle of repose of the cylindrical granules found in the experiment. The height of the granules' bed was found to be marginally higher, and the static angle of repose of the spherical granules was found to be marginally lower than that of the cylindrical granules. The bulk density of the spherical granules was about 1.20% lower than the cylindrical granules. As can be seen from these results, the behavior of cylindrical granules is close to that of cylindrical granules. At higher drum speeds and when the granules are subjected to high centrifugal forces in disk fertilizer spreaders, the behavior of the spherical granules is likely to be quite different from that of the cylindrical granules due to their shape. To determine this, experimental field and DEM simulation studies of the spreading of these granular organic fertilizers are needed.

This is important for an entire range of studies on the behavior and performance of bulk materials, e.g., spreading using centrifugal spreaders, granule separation, transport, and other questions.

## 4. Conclusions

It can be argued that after the experimental and DEM simulation studies on bone meal granules, it is sufficient to perform two experimental studies on (1) static compression to determine the modulus of elasticity of the granules and (2) friction between the granules and the contact surface of the equipment to determine the static and dynamic friction coefficients. Subsequently, three experimental and DEM simulation studies on the properties of the granules are sufficient; (3) the dynamic angle of repose and height of the granules' bed, (4) static angle of repose, and (5) poured bulk density are sufficient to test and confirm the remaining properties of the granule material and the interaction between the granules that have not been experimentally determined.

The spherical granules of the bone meal used in the simulation studies were found to have a diameter of 3.97 $\pm$ 0.07 mm; the diameter of the granules varied from 2.94 to 4.95 mm, with a distribution of granules close to the normal distribution.

The static compression tests on the bone meal granules showed that the static compression strength of the horizontally positioned granules was 29.81 N, and the calculated modulus of elasticity of the bone meal granules was 28.82 $\pm$ 5.29 MPa.

The static and dynamic coefficients of friction between the granules and the contacting surface were determined to be 0.28 for the static coefficient and 0.16 for the dynamic coefficient. Due to the heterogeneity of the material of the bone meal granules, a significant scatter in the values of the static coefficient of friction was found when compared to the scatter in the values of the dynamic coefficient of friction. These fertilizer properties were verified in DEM granule modeling studies. Experimental and DEM simulation studies for the evaluation of the dynamic angle of repose and the height of the granules' bed formed showed that the best visual agreement with the obtained values was achieved when the static coefficient of friction between granules was zero. Experimental and DEM simulation studies of the static angle of repose and the bulk density of the poured granules also fully confirmed these values of the interaction coefficients between the granules.

Experimental and simulation studies for the evaluation of the dynamic angle of repose, the granule pitch, the static angle of repose of the granules, and the bulk density of the granules showed that the coefficient of restitution between the granules was 0.60 and that the coefficient of restitution between the granules and the material of the study equipment was 0.45.

The diameter of the spherical granules used in the DEM simulation studies was 3.97 $\pm$ 0.07 mm, and their diameter distribution was close to the normal distribution.

It was found that spherical granules from the same raw material and with similar physical properties showed identical behavior compared to cylindrical granules. In addition, the dynamic angle of repose of the spherical granules was about +4.51%, and the height of the granules' bed was about +1.29% higher compared to the cylindrical ones. It was also found that the static angle of repose of spherical bone meal granules was about $-$2.64% lower than that of cylindrical granules.

Due to their shape, spherical granules' behavior in centrifugal spreaders can be assumed to be completely different from that of cylindrical granules. However, experimental and field studies on the spreading of these granular organic fertilizers are needed to determine this.

**Author Contributions:** Conceptualization, E.J., V.B. and R.M.; methodology, E.J., V.B., D.K. and R.M.; software, V.B. and R.M.; validation, E.J., V.B. and R.M.; formal analysis, E.J., V.B., D.K. and R.M.; investigation, E.J., V.B. and R.M.; data curation, E.J., V.B., D.K. and R.M.; writing—original draft preparation, E.J., V.B., D.K. and R.M.; writing—review and editing, E.J., V.B., D.K. and R.M.; visualization, E.J., V.B., D.K. and R.M.; supervision, E.J.; project administration, E.J.; funding acquisition, E.J., V.B., D.K. and R.M. All authors have read and agreed to the published version of the manuscript.

**Funding:** This research received no external funding.

**Conflicts of Interest:** The authors declare no conflicts of interest.

## References

1. Wang, Y.; Zhu, Y.; Zhang, S.; Wang, Y. What could promote farmers to replace chemical fertilizers with organic fertilizers? *J. Clean. Prod.* **2018**, *199*, 82–890. [CrossRef]
2. Yinyan, S.; Man, C.; Xiaochan, W.; Odhiambo, M.O.; Weimin, D. Numerical simulation of spreading performance and distribution pattern of centrifugal variable-rate fertilizer applicator based on DEM software. *Comput. Electron. Agric.* **2018**, *144*, 249–259. [CrossRef]
3. Balafoutis, A.T.; Koundouras, S.; Anastasiou, E.; Fountas, S.; Arvanitis, K. Life cycle Assessment of two vineyards after the application of precision viticulture techniques: A case study. *Sustainability* **2017**, *9*, 1997. [CrossRef]

4. Zeng, S.; Tang, H.; Luo, X.; Ma, G.; Wang, Z.; Zang, Y.; Zhang, M. Design and experiments of synchronous trenching, starting and fertilizing rice precision dry hole direct seeding machine. *J. Agric. Eng.* **2012**, *28*, 12–19.
5. Šarauskis, E.; Naujokienė, V.; Lekavičienė, K.; Kriaučiūnienė, Z.; Jotautienė, E.; Jasinskas, A.; Zinkevičienė, R. Application of granular and non-granular organic fertilizers in terms of energy, environmental and economic efficiency. *Sustainability* **2021**, *13*, 9740. [CrossRef]
6. Jalali, M.; Hurseresht, Z. Assessment of Mobile and Potential Mobile Trace Elements Extractability in Calcareous Soils Using Different Extracting Agents. *Front. Environ. Sci. Eng.* **2020**, *14*, 7. [CrossRef]
7. Gou, Y.; Li, H.; Wang, D.; He, H. Design and simulation optimization of a small variable fertilizer spreader based on EDEM. *J. Agric. Mech. Res.* **2022**, *44*, 65–71, 76.
8. Yang, L.; Chen, L.; Zhang, J.; Liu, H.; Sun, Z.; Sun, S.; Zheng, L. Fertilizer sowing simulation of a variable-rate fertilizer applicator based on EDEM. IFAC-Pap. *Line* **2018**, *51*, 418–423. [CrossRef]
9. Kweon, G.; Grift, T.E.; Miclet, D.; Virin, T.; Piron, E. Analysis and control of uniformity by the feed gate adaptation of a granular spreader. *J. Biosyst. Eng.* **2009**, *34*, 95–105.
10. Zhou, Y.C.; Yu, A.B.; Stewart, R.L.; Bridgwater, J. Microdynamic analysis of the particle flow in a cylindrical bladed mixer. *Chem. Eng. Sci.* **2004**, *59*, 1343–1364. [CrossRef]
11. Van Liedekerke, P.; Tijskens, E.; Dintwa, E.; Rioual, F.; Vangeyte, J.; Ramon, H. DEM simulations of the particle flow on a centrifugal fertilizer spreader. *Powder Technol.* **2009**, *190*, 348–360. [CrossRef]
12. Fulton, J. *Physical Properties of Granular Fertilizers and Impact on Spreading*; FABE-550.1; Ohioloine: Columbus, OH, USA, 2016.
13. Yule, I. The effect of fertilizer particle size on spread distribution. Adding to the Knowledge Base for the Nutrient Manager. *Agric. Food Sci.* **2011**, 1–9. Available online: https://api.semanticscholar.org/CorpusID:148567027 (accessed on 12 March 2024).
14. Yuan, F.; Yu, H.; Wang, L.; Shi, Y.; Wang, X.; Liu, H. Parameter Calibration and Systematic Test of a Discrete Element Model (DEM) for Compound Fertilizer Particles in a Mechanized Variable-Rate Application. *Agronomy* **2023**, *13*, 706. [CrossRef]
15. Bivainis, V.; Jotautienė, E.; Lekavičienė, K.; Mieldažys, R.; Juodišius, G. Theoretical and Experimental Verification of Organic Granular Fertilizer Spreading. *Agriculture* **2023**, *13*, 1135. [CrossRef]
16. Zeng, Z.; Ma, X.; Cao, X.; Li, Z.; Wang, X. Application status and prospect of discrete element method in agricultural engineering research. *J. Agric. Mach.* **2021**, *52*, 1–20.
17. Zhao, H.; Huang, Y.; Liu, Z.; Liu, W.; Zheng, Z. Applications of discrete element method in the research of agricultural machinery: A review. *Agriculture* **2021**, *11*, 425. [CrossRef]
18. Zeng, Z.W.; Chen, Y.; Long, Q. Simulation of cotyledon-soil dynamics using the discrete element method (DEM). *Comput. Electron. Agric.* **2020**, *174*, 105505. [CrossRef]
19. Liu, C.L.; Li, Y.N.; Song, J.N.; Ma, T.; Wang, M.M.; Wang, X.J.; Zhang, C. Performance analysis and experiment on fertilizer spreader with centrifugal swing disk based on EDEM. *Trans. Chin. Soc. Agric. Eng.* **2017**, *33*, 32–39.
20. Shmulevich, I. State of the art modeling of soil–tillage interaction using discrete element method. *Soil Tillage Res.* **2010**, *111*, 41–53. [CrossRef]
21. Liu, Z.D.; Wang, Q.J.; Li, H.W.; He, J.; Lu, C.Y.; Yu, C.C. Fertilizer injecting route analysis and test for air-blowing seed-fertilizer hole-applicator via CFD-DEM coupling. *Trans. Chin. Soc. Agric. Eng.* **2019**, *35*, 18–25.
22. Dun, G.; Mao, N.; Ji, X.; Zhang, F.; Ji, W. Optimal Design and Experiment of Corn-Overlapped Strip Fertilizer Spreader. *Appl. Sci.* **2023**, *13*, 2559. [CrossRef]
23. Zinkevičienė, R.; Jotautienė, E.; Jasinskas, A.; Kriaučiūnienė, Z.; Lekavičienė, K.; Naujokienė, V.; Šarauskis, E. Determination of Properties of Loose and Granulated Organic Fertilizers and Qualitative Assessment of Fertilizer Spreading. *Sustainability* **2022**, *14*, 4355. [CrossRef]
24. Dintwa, E.; Tijskens, E.; Olieslagers, R.; De Baerdemaeker, J.; Ramon, H. Calibration of a spinning disc spreader simulation model for accurate site specific fertilizer application. *Biosyst. Eng.* **2004**, *88*, 49–62.
25. Gallego, E.; Fuentes, J.M.; Ruiz, Á.; Hernández-Rodrigo, G.; Aguado, P.; Ayuga, F. Determination of mechanical properties for wood pelletgranules used in DEM simulations. *Int. Agrophys.* **2020**, *34*, 485–494. [CrossRef]
26. Ding, S.; Bai, L.; Yao, Y.; Yue, B.; Fu, Z.; Zheng, Z.; Huang, Y. Discrete element modelling (DEM) of fertilizer dual-banding with adjustable rates. *Comput. Electron. Agric.* **2018**, *152*, 32–39. [CrossRef]
27. Behjani, M.A.; Rahmanian, N.; Hassanpour, A. An investigation on the process of seeded granulation in a continuous drum granulator using DEM. *Adv. Powder Technol.* **2017**, *28*, 2456–2464. [CrossRef]
28. Olsson, U.; Engstrand, U.; Rupšys, P. *Statistical Methods Using SAS and MINITAB*; Lithuanian University of Agriculture: Kaunas, Lithuania, 2000.
29. Wypych, G. *Handbook of Polymers*; Elsevier: Amsterdam, The Netherlands, 2022.
30. Nouh, S.A.; KuShaari, K.; Keong, L.K.; Samsuri, S. Material characterization and inter/intra-particle validation for DEM simulation of urea coating process. *Particuology* **2024**, *88*, 32–48. [CrossRef]